Suppression of the charge-density-wave state in $Sr_{10}Ca_4Cu_{24}O_{41}$ by external pressure

C. A. Kuntscher,[1,*] A. Huber,[1] and M. Hücker[2]

[1]*Experimentalphysik 2, Universität Augsburg, D-86195 Augsburg, Germany*

[2]*Condensed Matter Physics & Materials Science Department, Brookhaven National Laboratory, Upton, New York 11973, USA*

(Received 9 January 2014; revised manuscript received 11 March 2014; published 17 April 2014)

The influence of external pressure on the charge-density-wave (CDW) ground state of the quasi-one-dimensional two-leg ladder compound $Sr_{10}Ca_4Cu_{24}O_{41}$ has been studied by optical reflectivity measurements as a function of temperature (10–300 K) and pressure P (0.3–4.3 GPa) over the spectral range 580–6000 cm^1. With increasing pressure the CDW transition temperature T_{CDW} decreases with the linear pressure coefficient ≈ -70 K/GPa, and above ≈ 3 GPa the CDW phase is suppressed at all temperatures. This behavior is similar to that in compounds $Sr_{14-x}Ca_xCu_{24}O_{41}$ with increasing Ca content x at ambient pressure, with the simple scaling $x \approx 3 \times P$(GPa). The size of the CDW gap decreases with increasing pressure, whereas the dimensionality of the high-temperature insulating phase in $Sr_{10}Ca_4Cu_{24}O_{41}$ within the ladder plane is hardly affected by external pressure.

DOI: 10.1103/PhysRevB.89.134510 PACS number(s): 71.45.Lr, 78.20.−e, 78.30.−j, 62.50.−p

I. INTRODUCTION

The cuprate spin ladder compounds have been the subject of intense experimental and theoretical research in recent years, because their layered structure, composed of quasi one-dimensional building blocks, positions these materials at the intersection between purely one and two-dimensional systems, where interesting physics can be expected [1,2]. There are high hopes that studies of the spin ladders may also further our understanding of the quasi two-dimensional cuprate high-temperature superconductors. Spin ladder compounds exhibit a number of exotic properties, as for example spin-charge separation [3], spin-gapped metallic state [4], as well as a competition between energetically close ground states, such as superconductivity [5] and insulating Wigner crystal phase (often called charge-density-wave phase) [6].

The structural unit cell of the quasi-one-dimensional compound $M_{14}(CuO_2)_{10}(Cu_2O_3)_7$ with M = La, Y, Sr, or Ca consists of two types of copper oxide layers that are parallel to the crystallographic a-c plane and alternate along the b axis: the Cu_2O_3 planes which contain the two-leg ladders, and planes containing CuO_2 chains with edge-shared CuO_4 plaquettes [2]. They belong to the class of low-dimensional transition-metal oxides with strong electronic correlations. The Cu moments on the rungs of the two-leg ladder form singlets. By means of Ca doping or application of hydrostatic pressure, the ladders can be doped with hole charge carriers. The current picture is that the doped holes are distributed such that a ladder rung is either doubly occupied by holes or empty. It was first predicted [1], and eventually experimentally confirmed [5], that hole doped ladders can become superconducting (SC). In particular, superconductivity with a T_C of 12 K was discovered in $Sr_{0.4}Ca_{13.6}Cu_{24}O_{41.8}$ at a pressure of 3 GPa [5]. However, the strong correlations between the holes allow for other ground states that compete with superconductivity, such as the mentioned charge-density-wave (CDW) order. The delicate balance between the SC and CDW states is not well understood. However, it is reminiscent of the competition between superconductivity and charge ordered states in the two-dimensional cuprates, as for example stripe order in La-based [7,8], and charge-density-wave order in Y-based materials [9,10]. This makes the spin ladder an important reference system for the overall understanding of the copper oxide materials.

The compound $La_6Ca_8Cu_{24}O_{41}$ is a Mott insulator, with an energy gap of approximately 2 eV in size, which can be doped with holes by substitution of La by Sr, as in $La_{6-y}Sr_yCa_8Cu_{24}O_{41}$. For the complete substitution of La by Sr the maximum hole doping of $n_h = 6$ holes per formula unit is reached and the average copper valence is +2.25. How the holes are distributed among the ladder and chain subsystems is an important issue, since it determines the physical properties. Related results from different techniques, including x-ray absorption and optical spectroscopy, are inconclusive [11–19]. The hole distribution can be tuned by changing the ratio between Sr and Ca in $Sr_{14-x}Ca_xCu_{24}O_{41}$ as well as by the application of pressure, and for high Ca concentrations and high pressure superconductivity is found.

In Ca free $Sr_{14}Cu_{24}O_{41}$ dc-resistivity, low-frequency dielectric spectroscopy, and optical spectroscopy revealed an insulator-to-insulator transition at about 210 K below which the holes in the ladders form an unconventional CDW ground state [6,20–23]. According to the frequency-dependent complex dielectric response Ca doping suppresses the CDW state: The transition temperature T_{CDW} decreases from 210 K for $x = 0$ to 7 K for $x = 9$ [22]. The size of the CDW energy gap Δ_{CDW} was determined from the suppression of spectral weight below Δ_{CDW} in the optical conductivity spectra for the polarization $\mathbf{E}$ of the radiation along the most conducting direction (i.e., c axis). It decreases from $\Delta_{CDW} = 112$ meV for $x = 0$ to 2.5 meV for $x = 9$ [22]. In contrast to these findings, a resonant x-ray scattering study has been able to identify charge order only in compounds with $10 \leqslant x \leqslant 12$, in addition to the $x = 0$ compound [24]. The existence of a CDW for the Ca content $x = 11$ is supported by an optical study [25].

Obviously, the ground state of the $Sr_{14}Cu_{24}O_{41}$ system responds very sensitively to Ca doping and external pressure. The substitution of Sr by Ca causes chemical pressure in the system due to the smaller ionic radius of the latter.

*christine.kuntscher@physik.uni-augsburg.de

According to x-ray diffraction experiments the main effect of both chemical and external pressure is a strong decrease in the lattice parameter b and hence a reduced distance between the ladder and chain layers increasing the interlayer coupling [26–28]. In a first attempt, the SC and CDW ground states have been included in a three-dimensional phase diagram with temperature, Ca content x, and pressure as the three variables [2,5,22,23,27,29–31]. However, this phase diagram can only be considered as preliminary, since not all combinations of the three variables have been investigated experimentally. In this paper we focus on the influence of external pressure on the CDW ground state in $Sr_{10}Ca_4Cu_{24}O_{41}$, which we study by optical reflectivity measurements as a function of temperature and pressure.

II. EXPERIMENT

The studied $Sr_{10}Ca_4Cu_{24}O_{41}$ single crystal was grown by the floating zone technique [32]. The mid-infrared reflectivity (580–6000 cm^{-1}) at low temperature and high pressure was measured using a home-built infrared microscope coupled to a Bruker Vertex 80/v FTIR spectrometer and maintained at the same vacuum conditions as the spectrometer, in order to avoid absorption lines of H_2O and CO_2 molecules. Thus, the parallel beam of the radiation from the interferometer can enter the IR microscope without passing a window. The scheme of the infrared microscope is depicted in Fig. 1. The setup can be operated either in reflection or in transmission mode, depending on the position of the movable mirror 1. The paths of the beam for both measuring geometries are symmetrical (see Fig. 1). A spherical mirror focuses the beam on the focal plane of the Schwarzschild objective (in reflection mode) or on the focal plane of the Schwarzschild condenser (in transmission mode). The infrared radiation is focused on the sample by all-reflecting home-made Schwarzschild objectives with a large working distance of about 55 mm and 14× magnification.

A diamond anvil cell (DAC) [33] equipped with type IIA diamonds suitable for infrared measurements was used to generate pressures up to 4.3 GPa. Finely ground CsI powder was chosen as quasihydrostatic pressure transmitting medium. The DAC was mounted on the cold finger of a continuous-flow helium cryostat (CryoVac KONTI) with two metallic rods, which allow mechanical access to the DAC lever arm mechanism. Thus, the pressure in the DAC could be changed *in situ* at arbitrary temperature. The pressure in the DAC was determined *in situ* by the standard ruby-fluorescence technique [34]. To this end, the ruby balls in the DAC are excited by a green laser with $\lambda = 532$ nm, and the ruby fluorescence

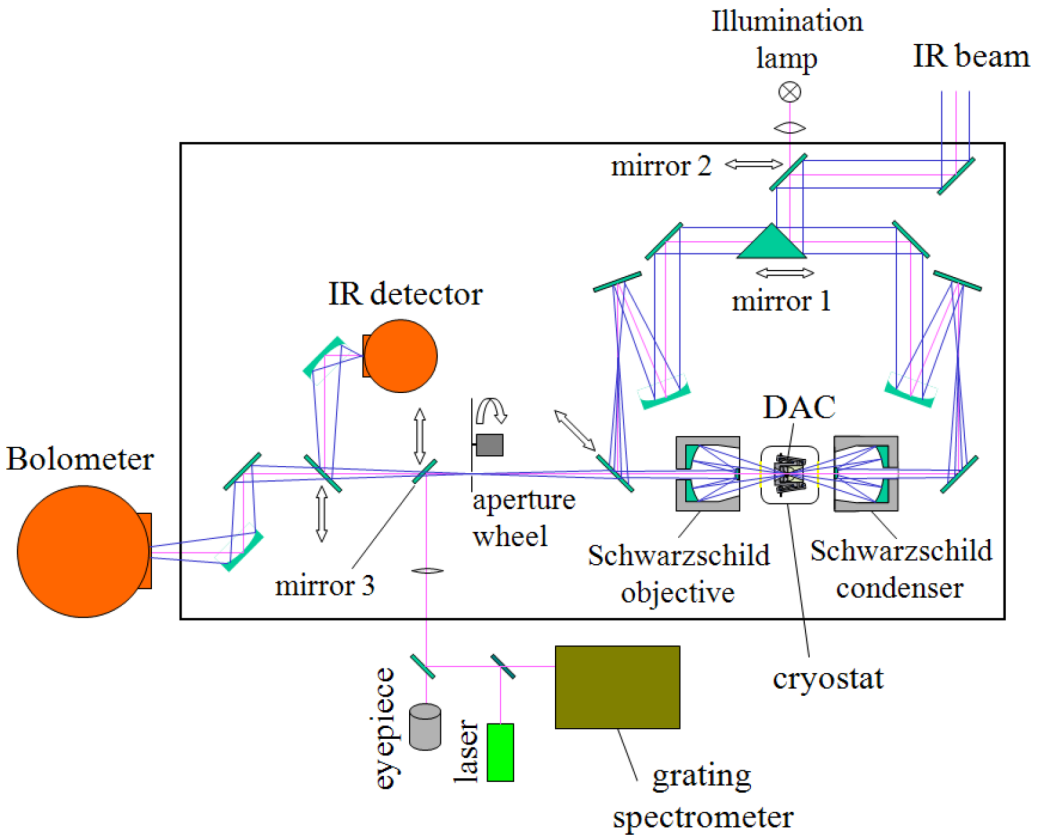

FIG. 1. (Color online) Scheme of the home-built infrared microscope coupled to a Bruker Vertex 80/v FTIR spectrometer for high-pressure and low-temperature optical reflectivity and transmission measurements. Depending on the position of mirror 1 the setup can be operated in either reflection or transmission mode. The radiation is focused on the sample by Schwarzschild objectives. For the visible inspection of the sample mirror 2 is moved, so that the light from the illumination lamp is passing to the sample, and additionally mirror 3 is moved to guide the light towards the eyepiece. For the *in situ* pressure determination the ruby balls in the DAC are excited by a green laser ($\lambda = 532$ nm), and the ruby fluorenscence spectra are recorded with a grating spectrometer. For polarization-dependent measurements a polarizer is added to the optical scheme.

spectra are recorded with a grating spectrometer. The direct observation of the sample is possible via the eyepiece or with a video camera (moving mirror 2 and 3, see Fig. 1). The above-described setup enables polarization-dependent transmission and reflectivity measurements over a broad frequency range (far-infrared to visible) for temperatures between ≈10 and 300 K, and pressures up to 20 GPa.

Details about the geometry of the reflectivity measurements and the Kramers-Kronig (KK) analysis of the reflectivity spectra $R_{s\text{-}d}$ at the sample-diamond interface can be found in our earlier publications [35,36]. For the KK analysis the reflectivity spectra were fitted with the Drude-Lorentz model, in order to extrapolate the missing low- and high-frequency parts of the spectra. Hereby, the dc resistivity data of $Sr_{11}Ca_3Cu_{24}O_{41}$ for $E\|c$ in Ref. [30] were taken into account for the low-frequency extrapolation. For the high-frequency extrapolation the reflectivity data of $Sr_{11}Ca_3Cu_{24}O_{41}$ at room temperature [11] were used for all studied temperatures and pressures. The multiphonon absorptions in the diamond anvil cause artifacts in the reflectivity spectra in the frequency range 1800–2700 cm^{-1}; therefore, the spectra were interpolated in this range according to the Drude-Lorentz fitting of the reflectivity spectra. All measurements were carried out with the polarization **E** of the radiation along the crystallographic c axis (ladder legs).

III. RESULTS AND DISCUSSION

The room-temperature reflectivity spectra $R_{s\text{-}d}$ of $Sr_{10}Ca_4Cu_{24}O_{41}$ at the diamond-sample interface are depicted in Fig. 2(a) for various pressures. At the lowest pressure (0.3 GPa) the reflectivity spectrum shows a plasma edge and phonon modes at around 550 cm^{-1}, consistent with published data [11]. The observation of a plasma edge at optical frequencies is not in contradiction to the insulating behavior found in electrical transport measurements, since the localization of the carriers due to disorder or electronic correlations is a low-energy phenomenon. The corresponding optical conductivity spectrum σ_1 [see Fig. 2(b)] contains considerable spectral weight in the studied frequency range, which can be attributed to excitations in the ladders [11]. With increasing pressure the plasma edge in the reflectivity spectrum shifts to higher frequencies and the overall optical conductivity increases. In analogy to the ambient-pressure results for $Sr_{14-x}Ca_xCu_{24}O_{41}$ with increasing Ca content, we interpret this increase of spectral weight in terms of a transfer of holes from the chain to the ladder subsystem [11].

To explore the pressure dependence of the CDW ground state, the reflectivity $R_{s\text{-}d}$ was measured for various pressures as a function of temperature down to 10 K (see Fig. 3). The opening of a CDW gap in the electronic band structure is manifested by an overall decrease and a change in slope of the reflectivity spectrum above 800 cm^{-1}, occurring at around 150 K at the lowest pressure [see Fig. 3(a)]. Taking the change in the slope of the reflectivity spectrum as the criterium for entering the CDW state, the CDW transition temperature T_{CDW} was determined as a function of pressure: With increasing pressure T_{CDW} decreases with the linear pressure coefficient of ≈−70 K/GPa, and at ≈3 GPa the CDW phase is completely

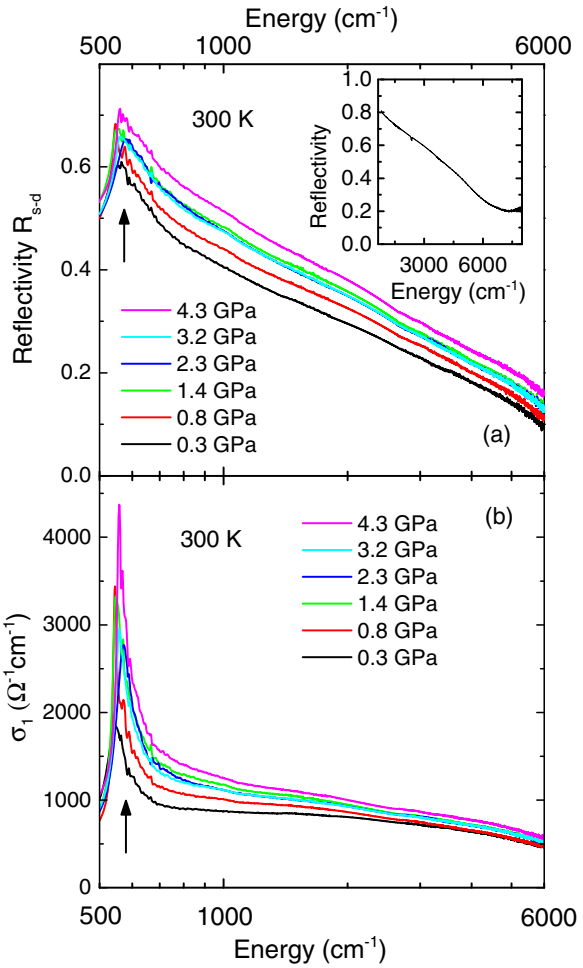

FIG. 2. (Color online) (a) Room-temperature reflectivity spectra $R_{s\text{-}d}$ and (b) corresponding optical conductivity spectra of $Sr_{10}Ca_4Cu_{24}O_{41}$ for $\mathbf{E}\|c$ for various applied pressures. The arrows mark the phonon mode region. The inset in (a) depicts the mid-infrared reflectivity spectrum of the free-standing sample, taken outside the DAC, for illustrating the plasma edge.

suppressed. Above 3 GPa the shape of the reflectivity spectrum with a plasma edge is retained at all temperatures, and the temperature-induced changes are small. Based on the pressure and temperature evolution of the reflectivity data we propose the temperature-pressure phase diagram of $Sr_{10}Ca_4Cu_{24}O_{41}$ as shown in Fig. 4, including the low-temperature CDW phase and the high-temperature (HT) insulating phase [22].

The optical conductivity spectra σ_1 as obtained by KK analysis of the reflectivity spectra are depicted in Fig. 5. At the lowest applied pressure (0.3 GPa), the optical conductivity decreases below 3000 cm^{-1} for temperatures below 150 K, which signals the opening of the CDW gap [see Fig. 5(a)]. This decrease becomes more pronounced for lower temperatures. At the lowest temperature one observes a pronounced increase in the optical conductivity above 700 cm^{-1}, but there is no peak structure corresponding to single-particle excitations across the CDW gap, which could serve as an energy scale for the CDW gap. We therefore use the increase in the optical conductivity above 700 cm^{-1} to estimate the size of the CDW

gap to $\Delta_{CDW} \approx 87$ meV at 0.3 GPa, in analogy to Ref. [22]. The suppression of the CDW phase with increasing pressure is also seen in the optical conductivity spectra (see Fig. 5), as the temperature-induced suppression in the frequency range <3000 cm^{-1} gradually diminishes with increasing pressure and disappears for pressures above ≈ 3 GPa. Furthermore, with increasing pressure the onset of the strong increase in the optical conductivity observed at 10 K and 0.3 GPa shifts to frequencies below the studied frequency range. Hence, the decrease of Δ_{CDW} with increasing pressure cannot be determined based on the present data.

Next we compare the effect of external pressure on the CDW state with that of increasing Ca content x. According to the temperature dependence of the complex dielectric response [22] the CDW transition temperature decreases with increasing x and reaches the value $T_{CDW} = 20$ K for $x = 9$. These ambient-pressure results as a function of Ca content are included in the phase diagram in Fig. 4 [37]. From the comparison of the two data sets we obtain the simple scaling $x \approx 3 \times P$(GPa) between the Ca content x and the applied pressure P.

To drive $Sr_{14-x}Ca_xCu_{24}O_{41}$ towards a SC state, both a high Ca content and external pressure are needed [5]. Ca doping induces a more two-dimensional charge distribution in the ladder subunit according to x-ray absorption measurements [12]. It was suggested that external pressure diminishes the electronic correlations, which causes a HT insulating phase even for high Ca doping, and increases the dimensionality of the system further to two dimensional within the a-c ladder plane [22]. Hence, also the SC state is expected to be less anisotropic within the ladder planes. A comparison of the HT reflectivity spectra for the two polarization directions $\mathbf{E}\|c$ (i.e., along the ladder legs) and $\mathbf{E}\|a$ (i.e., along the ladder rungs) can serve as an indicator for the dimensionality of

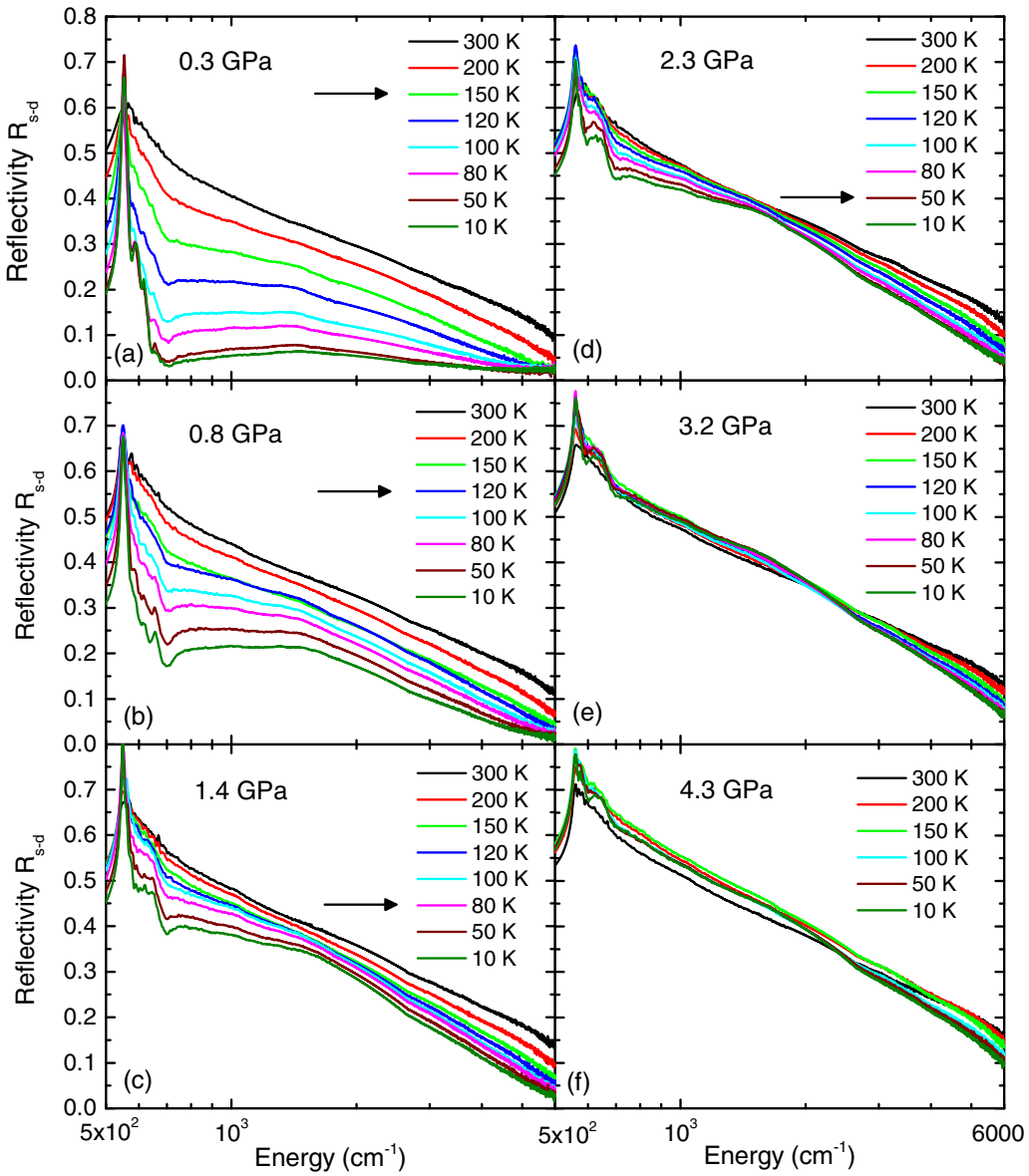

FIG. 3. (Color online) Reflectivity spectra $R_{s\text{-}d}$ of $Sr_{10}Ca_4Cu_{24}O_{41}$ for $\mathbf{E}\|c$ as a function of temperature for various pressures. The arrows mark the transition temperature T_{CDW}, as determined from the change in the slope of the reflectivity spectra.

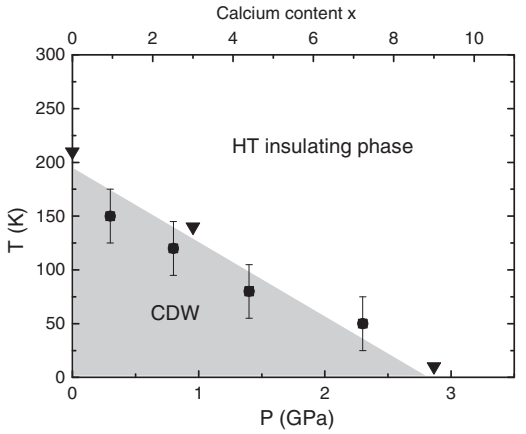

FIG. 4. Temperature-pressure phase diagram of $Sr_{10}Ca_4Cu_{24}O_{41}$ showing the high-temperature (HT) insulating phase and the charge-density-wave (CDW) phase. The filled squares mark the CDW transition temperature T_{CDW} as extracted from the pressure- and temperature-dependent reflectivity spectra. The filled triangles mark T_{CDW} for ambient-pressure $Sr_{14-x}Ca_xCu_{24}O_{41}$ as a function of Calcium content x (upper horizontal axis) from Ref. [22].

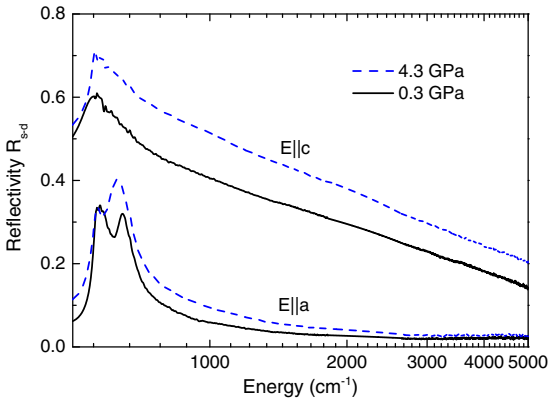

FIG. 6. (Color online) Room-temperature reflectivity spectra of $Sr_{10}Ca_4Cu_{24}O_{41}$ for the two polarization directions $\mathbf{E}\|c$ and $\mathbf{E}\|a$ at low (0.3 GPa) and high (4.3 GPa) pressure.

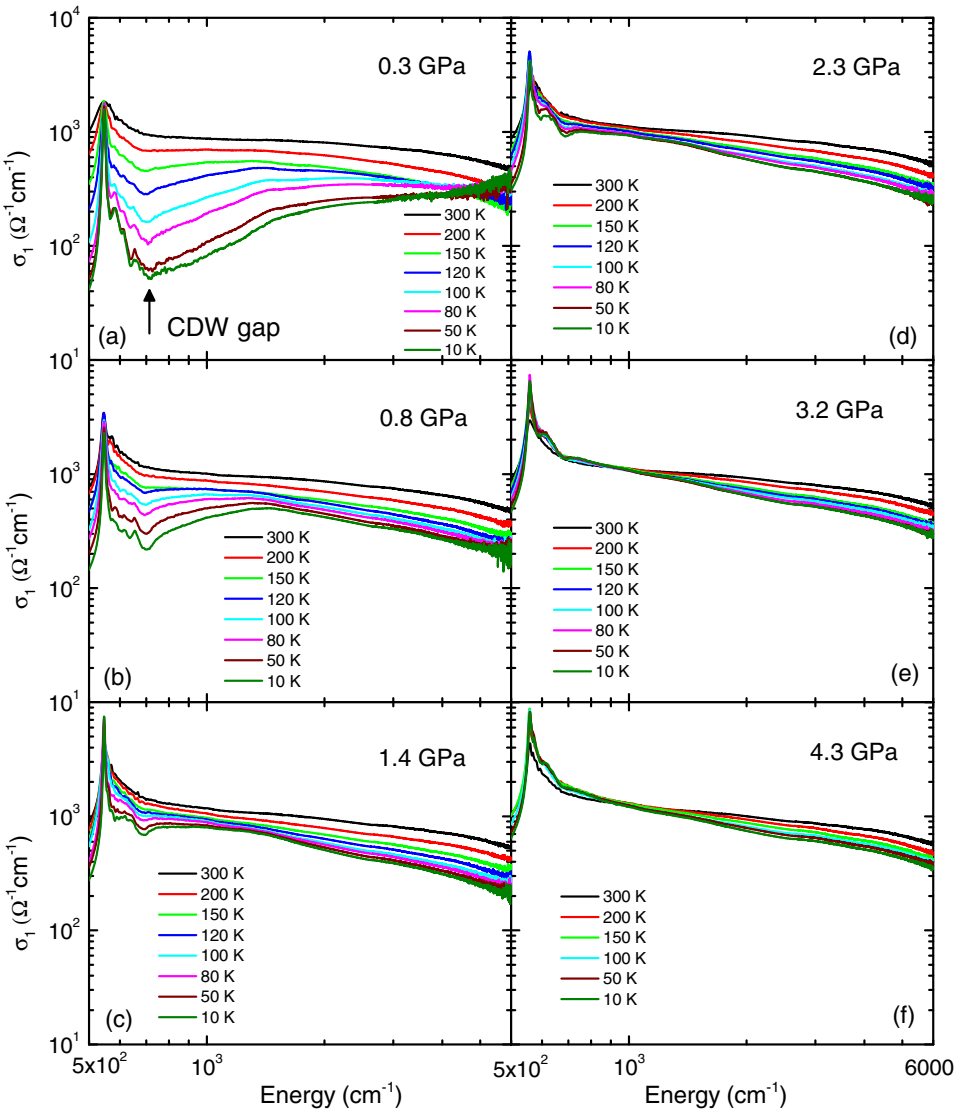

FIG. 5. (Color online) Real part of the optical conductivity σ_1 of $Sr_{10}Ca_4Cu_{24}O_{41}$ for $\mathbf{E}\|c$ as a function of temperature for various pressures.

the HT insulating phase within the ladder plane. We thus depict in Fig. 6 the room-temperature reflectivity spectra of $Sr_{10}Ca_4Cu_{24}O_{41}$ for $\mathbf{E}\|c,a$ and for the lowest (0.3 GPa) and highest (4.3 GPa) pressure. For the polarization direction $\mathbf{E}\|a$ the overall reflectivity is considerably lower as compared to $\mathbf{E}\|c$ and it contains two pronounced peaks at low frequencies due to phonon excitations. For an estimate of the degree of anisotropy we use the ratio $R_{s\text{-}d}(\mathbf{E}\|c)/R_{s\text{-}d}(\mathbf{E}\|a)$ of the reflectivity spectra above 1000 cm^{-1}, i.e., well above the phonon excitations; the ratio amounts to about 10. With increasing pressure the overall reflectivity increases slightly for both polarization directions, although the reflectivity ratio $R_{s\text{-}d}(\mathbf{E}\|c)/R_{s\text{-}d}(\mathbf{E}\|a)$ is unchanged. Obviously, the material remains highly anisotropic within the a-c plane up to the highest applied pressure. It seems that the dimensionality of the HT insulating phase is only slightly affected by external pressure for such a low Ca content. Also for high Ca contents the anisotropic character of the HT insulating state is preserved under external pressure, as demonstrated by the pressure dependence of the resistivity ratio ρ_a/ρ_c for $Sr_{2.5}Ca_{11.5}Cu_{24}O_{41}$ at room temperature [31] and by the pressure-dependent lattice constants in $Sr_{0.4}Ca_{13.6}Cu_{24}O_{41}$ [28]. The robustness of the anisotropic nature of the HT insulating state under pressure thus seems to be common to all compounds $Sr_{14-x}Ca_xCu_{24}O_{41}$.

IV. CONCLUSIONS

In conclusion, from our pressure- and temperature-dependent optical reflectivity data on $Sr_{10}Ca_4Cu_{24}O_{41}$ we infer a linear decrease of the CDW transition temperature T_{CDW}, with a linear pressure coefficient ≈ -70 K/GPa. Above ≈ 3 GPa the CDW phase is completely suppressed. By comparing the pressure dependence of T_{CDW} with the ambient-pressure values of T_{CDW} in the compounds $Sr_{14-x}Ca_xCu_{24}O_{41}$ for various Ca contents x, we find the simple scaling $x \approx 3 \times P$(GPa) between x and the applied pressure P. The size of the CDW gap decreases with increasing pressure. The HT insulating phase in $Sr_{10}Ca_4Cu_{24}O_{41}$ preserves its anisotropy within the ladder plane up to the highest applied pressure.

ACKNOWLEDGMENTS

We thank K. Syassen for providing valuable information about the optical design of the homemade infrared microscope and A. Pashkin for the optical design and construction of the homemade infrared microscope. This work is financially supported by the DFG (KU 1432/6-1). Work at Brookhaven was supported by the U.S. Department of Energy (DOE), under Contract No. DE-AC02-98CH10886.

[1] E. Dagotto and T. M. Rice, Science **271**, 618 (1996).
[2] T. Vuletic, B. Korin-Hamzic, T. Ivek, S. Tomic, B. Gorshunov, M. Dressel, and J. Akimitsu, Phys. Rep. **428**, 169 (2006).
[3] B. J. Kim, H. Koh, E. Rotenberg, S.-J. Oh, H. Eisaki, N. Motoyama, S. Uchida, T. Tohyama, S. Maekawa, Z.-X. Shen *et al.*, Nat. Phys. **2**, 397 (2006).
[4] E. Dagotto, J. Rieira, and D. Scalapino, Phys. Rev. B **45**, 5744 (2003).
[5] M. Uehara, T. Nagata, J. Akimitsu, H. Takahashi, N. Mori, and K. Kinoshita, J. Phys. Soc. Jpn. **65**, 2764 (1996).
[6] P. Abbamonte, G. Blumberg, A. Rusydi, A. Gozar, P. G. Evans, T. Siegrist, L. Venema, H. Eisaki, E. D. Isaacs, and G. A. Sawatzky, Nature (London) **431**, 1078 (2004).
[7] J. M. Tranquada, J. D. Axe, N. Ichikawa, A. R. Moodenbaugh, Y. Nakamura, and S. Uchida, Phys. Rev. Lett. **78**, 338 (1997).
[8] M. Hücker, M. v. Zimmermann, G. D. Gu, Z. J. Xu, J. S. Wen, G. Xu, H. J. Kang, A. Zheludev, and J. M. Tranquada, Phys. Rev. B **83**, 104506 (2011).
[9] G. Ghiringhelli, M. L. Tacon, M. Minola, S. Blanco-Canosa, C. Mazzoli, N. B. Brookes, G. M. D. Luca, A. Frano, D. G. Hawthorn, F. He *et al.*, Science **337**, 821 (2012).
[10] J. Chang, E. Blackburn, A. T. Holmes, N. B. Christensen, J. Larsen, J. Mesot, R. Liang, D. A. Bonn, W. N. Hardy, A. Watenphul *et al.*, Nat. Phys. **8**, 871 (2012).
[11] T. Osafune, N. Motoyama, H. Eisaki, and S. Uchida, Phys. Rev. Lett. **78**, 1980 (1997).
[12] N. Nücker, M. Merz, C. A. Kuntscher, S. Gerhold, S. Schuppler, R. Neudert, M. S. Golden, J. Fink, D. Schild, S. Stadler, V. Chakarian, J. Freeland, Y. U. Idzerda, K. Conder, M. Uehara, T. Nagata, J. Goto, J. Akimitsu, N. Motoyama, H. Eisaki, S. Uchida, U. Ammerahl, and A. Revcolevschi, Phys. Rev. B **62**, 14384 (2000).
[13] Y. Piskunov, D. Jerome, P. Auban-Senzier, P. Wzietek, and A. Yakubovsky, Phys. Rev. B **72**, 064512 (2005).
[14] A. Rusydi, M. Berciu, P. Abbamonte, S. Smadici, H. Eisaki, Y. Fujimaki, S. Uchida, M. Rübhausen, and G. A. Sawatzky, Phys. Rev. B **75**, 104510 (2007).
[15] E. Kabasawa, J. Nakamura, N. Yamada, K. Kuroki, H. Yamazaki, M. Watanabe, J. D. Denlinger, S. Shin, and R. C. C. Perera, J. Phys. Soc. Jpn. **77**, 034704 (2008).
[16] C. Ma, Y. X. Yang, L. J. Zeng, Y. Zhang, L. L. Wang, L. Chen, R. Xiong, J. Shi, and J. Q. Li, J. Phys.: Condens. Matter **21**, 215606 (2009).
[17] G. Deng, V. Pomjakushin, V. Petříček, E. Pomjakushina, M. Kenzelmann, and K. Conder, Phys. Rev. B **84**, 144111 (2011).
[18] V. Ilakovac, C. Gougoussis, M. Calandra, N. B. Brookes, V. Bisogni, S. G. Chiuzbaian, J. Akimitsu, O. Milat, S. Tomić, and C. F. Hague, Phys. Rev. B **85**, 075108 (2012).
[19] M.-J. Huang, G. Deng, Y. Y. Chin, Z. Hu, J.-G. Cheng, F. C. Chou, K. Conder, J.-S. Zhou, T.-W. Pi, J. B. Goodenough, H.-J. Lin, and C. T. Chen, Phys. Rev. B **88**, 014520 (2013).
[20] B. Gorshunov, P. Haas, T. Room, M. Dressel, T. Vuletic, B. Korin-Hamzic, S. Tomic, J. Akimitsu, and T. Nagata, Phys. Rev. B **66**, 060508 (2002).
[21] G. Blumberg, P. Littlewood, A. Gozar, B. S. Dennis, N. Motoyama, H. Eisaki, and S. Uchida, Science **297**, 584 (2002).
[22] T. Vuletic, B. Korin-Hamzic, S. Tomic, B. Gorshunov, P. Haas, T. Room, M. Dressel, J. Akimitsu, T. Sasaki, and T. Nagata, Phys. Rev. Lett. **90**, 257002 (2003).
[23] T. Vuletic, T. Ivek, B. Korin-Hamzic, S. Tomic, B. Gorshunov, P. Haas, M. Dressel, J. Akimitsu, T. Sasaki, and T. Nagata, Phys. Rev. B **71**, 012508 (2005).

[24] A. Rusydi, P. Abbamonte, H. Eisaki, Y. Fujimaki, G. Blumberg, S. Uchida, and G. A. Sawatzky, Phys. Rev. Lett. **97**, 016403 (2006).
[25] T. Osafune, N. Motoyama, H. Eisaki, S. Uchida, and S. Tajima, Phys. Rev. Lett. **82**, 1313 (1999).
[26] E. M. McCarron, M. A. Subramanian, J. C. Calabrese, and R. L. Harlow, Mat. Res. Bull. **23**, 13551988).
[27] M. Isobe, T. Ohta, M. Onoda, F. Izumi, S. Nakano, J. Q. Li, Y. Matsui, E. Takayama-Muromachi, T. Matsumoto, and H. Hayakawa, Phys. Rev. B **57**, 613 (1998).
[28] S. Pachot, P. Bordet, R. J. Cava, C. Chaillout, C. Darie, M. Hanfland, M. Marezio, and H. Takagi, Phys. Rev. B **59**, 12048 (1999).
[29] C. Hess, C. Baumann, U. Ammerahl, B. Büchner, F. Heidrich-Meisner, W. Brenig, and A. Revcolevschi, Phys. Rev. B **64**, 184305 (2001).
[30] N. Motoyama, H. Eisaki, S. Uchida, N. Takeshita, N. Mori, T. Nakanishi, and H. Takahashi, Europhys. Lett. **58**, 758 (2002).
[31] T. Nagata, M. Uehara, J. Goto, J. Akimitsu, N. Motoyama, H. Eisaki, S. Uchida, H. Takahashi, T. Nakanishi, and N. Mori, Phys. Rev. Lett. **81**, 1090 (1998).
[32] U. Ammerahl and A. Revcolevschi, J. Cryst. Growth **197**, 825 (1999).
[33] R. Keller and W. B. Holzapfel, Rev. Sci. Instrum. **48**, 517 (1977); G. Huber, K. Syassen, and W. B. Holzapfel, Phys. Rev. B **15**, 5123 (1977).
[34] H. K. Mao, J. Xu, and P. M. Bell, J. Geophys. Res. **91**, 4673 (1986).
[35] A. Pashkin, M. Dressel, and C. A. Kuntscher, Phys. Rev. B **74**, 165118 (2006).
[36] C. A. Kuntscher, S. Frank, A. Pashkin, M. Hoinkis, M. Klemm, M. Sing, S. Horn, and R. Claessen, Phys. Rev. B **74**, 184402 (2006).
[37] Please note that in Refs. [24] and [25] a different dependence of the CDW on the Ca content was found.